Quantitative Real-Time PCR: Fluorescent Probe Options and Issues

Marcia J. Holden[1] (✉) · Lili Wang[2]

[1]National Institute of Standards and Technology, Biochemical Science Division,
 100 Bureau Drive, Mail Stop 8311, Gaithersburg, MD 20899, USA
 marcia.holden@nist.gov

[2]National Institute of Standards and Technology, Biochemical Science Division,
 100 Bureau Drive, Mail Stop 8312, Gaithersburg, MD 20899, USA

Abstract Fluorescence has played a vital role in the development of polymerase chain reaction (PCR)-based DNA amplification. In qualitative PCR, an end point reaction, the amplified DNA, is visualized using DNA intercalating fluorescent dyes. Creative uses of nucleotide probes with fluorescent tags have been developed for real-time quantitative PCR. These probes take advantage of the behavior and properties of fluorophores. There are advantages and disadvantages to various probe types as well as design considerations. Attention to these issues will help in the development of robust and accurate DNA quantification using real-time PCR.

Keywords FRET · Hybridization probe · Molecular beacon · Real-time quantitative PCR · Scorpion primer · SYBR Green I · TaqMan probe

Abbreviations
Ct   Cycle threshold
CTAB Cetyltrimethylammonium bromide
DNA   Deoxyribonucleic acid
FRET Fluorescence resonance energy transfer
PCR   Polymerase chain reaction
T_m Melting temperature

1
PCR

The polymerase chain reaction (PCR) has become one of the most important tools in molecular biology in the last 30 years, with rapidly expanding uses in areas such as gene expression, disease detection and monitoring, species identification, forensics, single nucleotide polymorphisms, mutation detection, and evolutionary studies. The core of the technology, first developed in 1985 [1], is copying of specific sequences of DNA using the enzyme DNA polymerase in conjunction with primers (single-stranded DNA consisting of 20 to 25 bases) that match the DNA sequence at each end of the region to be amplified. The reaction mixture consists of the DNA polymerase, two primers (one for each strand of DNA), individual nucleotide triphosphates (building blocks for the copied DNA), buffer (with salts and additives), and template DNA. This reaction mixture goes through a temperature cycle wherein the double-stranded DNA is denatured at 95 °C into single strands by breaking of the hydrogen bonds between the bases. The temperature is lowered so that the primers, in high concentrations, can bind to the matching sequence on the template DNA. When the primers have bound then DNA polymerase utilizes that primer position as a place to recreate the double strand. The enzyme incorporates nucleotides to the primer with the order dictated by the sequence of the template DNA. This constitutes a single cycle of amplification. In the subsequent cycles the primers can bind to template DNA or to a previously amplified DNA fragment called an amplicon. In every cycle, in theory, it is possible to copy every previously amplified fragment of DNA, and reactions frequently involve 30 to 50 cycles. Billions to trillions of copies are produced which are easily visualized, for example, by electrophoresis in an agarose gel in the presence of ethidium bromide, which fluoresces upon intercalation in the DNA, or by capillary electrophoresis using a dye-labeled primer.

Two technological developments were implemented to increase the utility of the PCR. The first was the adoption of the thermostable DNA polymerase [2]. DNA polymerase would normally be degraded by heating to 95 °C and so the reaction had to be stopped during each cycle to add more polymerase. Thermostable DNA polymerases with a variety of properties have been isolated and cloned from thermal vent microbes whose enzymes must survive the high temperatures in which the organisms live. The second development was the creation of superior heat blocks. Precise temperature control and rapid temperature cycling were important for consistent results. At this stage of development PCR provided qualitative information, the accuracy of which was dependent on good design of the PCR protocol and the quality of the DNA template. Among the most important components are the specificity of the primers and the choice of the thermocycling temperatures. Primers with sequence similarity to other regions of DNA will result in mul-

tiple products. Temperatures for the annealing phases, if too low, can also lead to nonspecific amplification.

2
Real-Time Quantitative PCR (rt-Q-PCR)

Fluorescence in the form of ethidium bromide intercalated into DNA amplicons was important to visualize products in qualitative PCR, but fluorescence serves a vital role in quantitative PCR detection strategies as well. Instrumentation utilizing CCD cameras to measure fluorescence signals in every reaction and in each cycle of PCR opened the door to quantitative real-time PCR. Equipment manufacturers have developed a variety of platforms with various optical and heating/cooling options combined with plastic tubes, 96/384-well plates, or glass capillaries for holding the reactions. The speed of a completed protocol and the ability to monitor it in real time has driven different approaches. Machines vary in their ability to support the use of the proliferating fluorescence detection options and the ability to multiplex (more than one PCR reaction in each tube). Determining the needs of a laboratory and investigating the capabilities of each platform before purchase is therefore important.

The Q-PCR reaction mixture has the same components as a qualitative reaction with the addition of a detection probe, either DNA intercalating fluorescent dyes or specific single-stranded DNA with covalently linked fluorophore with or without an acceptor. The optimization of the reaction (concentrations of reaction components, timing, temperature) is as important for quantitative as qualitative PCR. It is out of the scope of this chapter to discuss in detail the many aspects of the PCR that must be considered during development and validation of a specific protocol, and instead we will focus on the fluorescent probe options and issues. Recent comprehensive sources of information include two volumes dedicated to quantitative PCR [3, 4].

Q-PCR real-time platforms monitor the fluorescence signal at some point during each PCR cycle, the timing being dependent on the nature of the fluorescent probe type used in the reaction (Fig. 1). Initially the signal is below a preselected baseline or threshold that is set above background noise, as there are few amplicons contributing to the signal (lag phase). But as the number of completed cycles increases the number of amplicons, the fluorescence signal will cross this threshold during the beginning of the log phase of the amplification. In later cycles a plateau is reached where the signal is relatively constant. No additional signal is generated for several possible reasons including exhaustion of the reagents. The amplification cycle at which the fluorescence in a particular reaction crosses the selected threshold is known as the cycle threshold, or Ct, and is in the early log phase of amplification. The initial copy number of target DNA sequences added to the reaction deter-
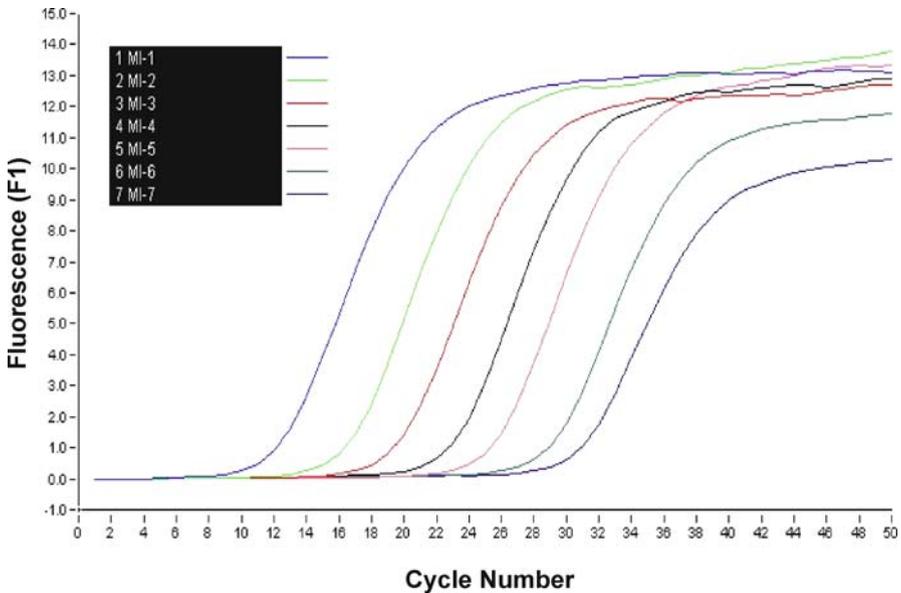
Fig. 1 Quantitative real-time amplification plot of a representative standard curve (tenfold dilutions of a plasmid). The insert graph is a plot of the Ct values vs the log of the concentration where the slope of the curve is –3.386

mines when that threshold is reached, all other things being equal. The Ct value is inversely proportional to the concentration of DNA targets. This is the basis of quantitation. Absolute quantitation involves the use of DNA or RNA standards, validated for the specific detection. An amplification efficiency of 100% equals a doubling of the number of amplicons in every cycle. Plots of the Ct values versus the log of the concentration of the target will yield a curve with a slope of [–3.32] when efficiency is equal to 100%. Two DNA samples or standards that differ in concentration by tenfold will have Ct values that differ by 3.3 cycles. Figure 1 shows the change in fluorescence for a series of tenfold dilutions of a plasmid. A plot of this data gives a slope of –3.386, for an efficiency of 97.4%.

3
Fluorescence Detection in Quantitative PCR: Nonspecific Detection

Fluorescence detection methods are utilized in real-time PCR due to the need for high sensitivity and a large dynamic range [5, 6]. The first attempts utilized ethidium bromide again as the source of fluorescence [7, 8]. SYBR Green I, which binds to the minor groove of the DNA double helix, has replaced ethidium bromide as an intercalating fluorescent dye [9, 10]. SYBR

Green I and related molecules represent a detection strategy that is non-specific, as any double-stranded DNA will bind SYBR Green. Therefore, the specificity of the PCR becomes an important issue. Amplification artifacts, such as primer dimers, will add to the signal [11, 12]. Running a melting protocol at the end of the amplification cycle protocol should help in validating the specificity of the reaction.

While it is a simple strategy for the detection of PCR amplicons, in practice the use of SYBR Green I is not necessarily straightforward. Diluted SYBR Green I can be stable for up to 3 weeks, but its breakdown products can be inhibitory to PCR and are increased by alkaline conditions [13]. The dye itself can be inhibitory depending on the concentration [6] and can affect the optimum magnesium concentration [13]. Additives may be necessary to optimize the reaction. SYBR Green I can also affect the melting temperature (T_m) of the products or even whether melting curve analysis can detect the product at all [14]. While SYBR Green has been used for multiplexing in cases where the T_m values of the products are sufficiently different to distinguish the amplicons, Giglio et al. [15] caution that there can be preferential dye binding to specific fragments. Further, some new versions of SYBR Green I introduced very recently address some of the problems noted above. Also a recent investigation into the use of the dye SYTO9 suggests that it might be a more stable and predictable alternative to SYBR Green I [14].

Nonspecific DNA intercalating/binding dyes offer a cost saving over specific fluorescent probes, discussed below, when running quantitative PCR assays. Alternatives to dyes, such as labeled primers, may not justify the cost (over the dyes), but they offer the possibility of multiplexing, that is, more than one PCR per tube.

4
Fluorescence Detection in Quantitative PCR: Specific Detection

All of the rest of the fluorescence detection strategies involve the use of oligonucleotide probes, complementary to a portion of the amplified target, which offer specificity. These oligonucleotide probes contain both a fluorophore donor and an acceptor (emissive or nonemissive) that interact through a fluorescence resonance energy transfer (FRET) mechanism [16–20]. When compared to the DNA binding dyes, fluorophores linked to oligonucleotides offer higher sequence specificity and are less susceptible to contamination, such as primer–dimer formation in the case of SYBR Green I [11, 12], and are somewhat easier for the detection of single nucleotide polymorphisms [18, 21, 22].

FRET is the underlying mechanism for various real-time PCR methods employing a variety of probe design tactics (Fig. 2) including TaqMan probes [19, 23], molecular beacons [16, 24, 25], hybridization probes [26, 27],
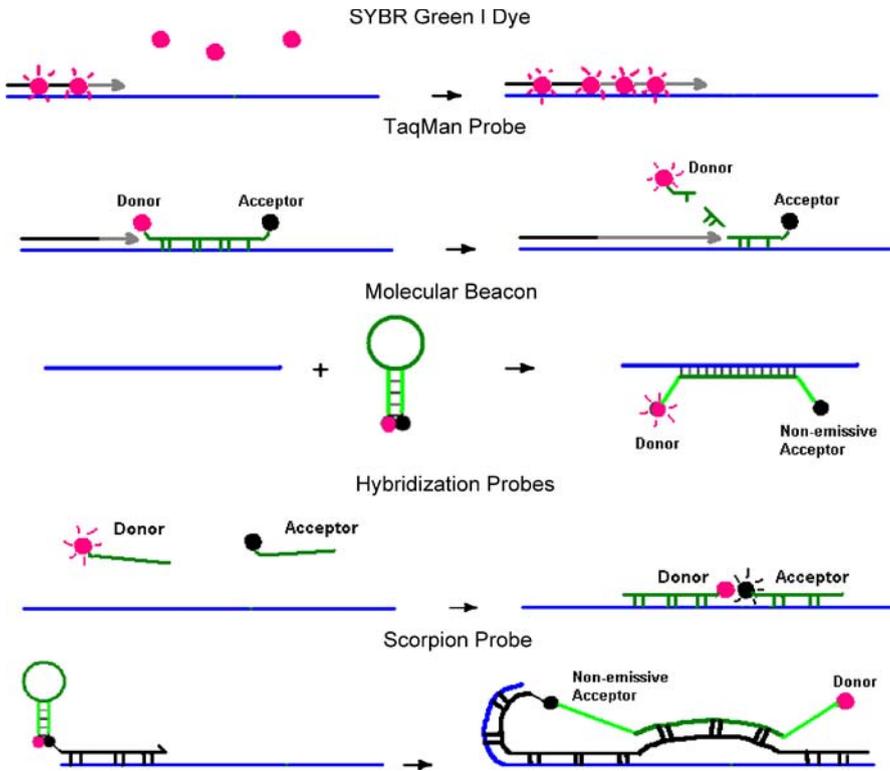
Fig. 2 Depictions of the more commonly used types of fluorescent detection probes used in quantitative real-time PCR

Scorpion primers [28], and strategies where fluorescence is quenched by neighboring nucleotides [18, 29]. FRET occurs between an energy donor and a suitable energy acceptor as a result of long-range dipole–dipole interactions between the two fluorophores. This type of energy transfer can take place over separation distances of 20 to 90 Å [30]. Contact quenching comes about when the donor and acceptor/quencher are in very close contact and quenching is more efficient than that of FRET with the same donor–acceptor pair [31]. The efficiency of FRET depends on the overlap of the emission spectra of the donor and the absorption spectra of the acceptor, whereas contact quenching does not.

4.1
Molecular Beacons

Because of the probe design strategy, molecular beacons generally give low initial fluorescence background. These probes are composed of a stem–loop structure. The loop portion contains the sequence for hybridization to the

amplified target while the stem is a double-stranded sequence complementary only to itself and not the target. The stem structure of the molecular beacons warrants efficient fluorescence contact quenching by the proximal acceptor. Upon hybridization to the amplified templates during PCR, donor fluorescence enhancement occurs due to the large separation distance between the donor and the acceptor. The molecular beacon is displaced from the target strand by DNA polymerase during the elongation phase of amplification. The donor–acceptor pair can have a significant impact on the T_m of the probe and should be considered in addition to the contribution of the nucleotides themselves [31]. This is particularly important because there is a competition between the formation of the stem and the binding of the loop sequence to the target DNA.

4.2
TaqMan Probe

The first of the current generation of real-time quantitative PCR assays combined a dual-labeled fluorogenic probe, TaqMan, with the use of the $5' \rightarrow 3'$ exonuclease activity of Taq DNA polymerase [23] and this approach remains the most popular option. By comparison to probes such as molecular beacons, TaqMan probes give much higher background signals in that the intramolecular separation distance between a donor and an acceptor in the unhybridized state results in only partial donor signal reduction. The random coil behavior brings the acceptor into the range of the donor for FRET. The amount of resonance energy transfer is considerably lower than in the case of the molecular beacon, because of the lack of the stem to bring the donor and acceptor into close proximity when not bound to the template DNA/amplicons. During PCR, TaqMan probes are hybridized to the amplicons and subsequently cleaved for removal from the templates by $5' \rightarrow 3'$ exonuclease activity of the Taq polymerase [32]. As a result, donor fluorescence enhancement takes place because of the cleavage of the donor fluorophore from the oligonucleotide probe, and therefore separation from the acceptor fluorophore. An assumption in these assays is that cleavage of the TaqMan probe is efficient.

Some modifications have been developed to address the background issue with TaqMan probes. For instance, a $3'$ minor groove binder (MGB, 1,2-dihydro-(3H)-pyrrolo[3,2-e]indole-7-carboxylate) is added to the conventional TaqMan probe design to enhance the binding affinity of short TaqMan MGB probes (8–16 mers) to their templates [33, 34]. In comparison to the conventional TaqMan probes, the short TaqMan MGB probes give much lower background signals due to the relatively short intramolecular separation distance between a donor and an acceptor in the unhybridized state. The short probe lengths warrant their use in mutation detections [35]. Their sensitivity in that respect can cause problems unless possible mismatches are well understood [36]. Other strategies for shortening probe length include the

use of locked nucleic acids (LNAs) incorporated into oligonucleotides [37]. LNAs are nucleic acid analogs with an O2 to C4 methylene linkage that has the effect of reducing conformational flexibility and raising the T_m of the oligonucleotide.

4.3
Hybridization FRET Probes

Hybridization FRET probes are composed of two separate oligonucleotides with one fluorophore attached to the $3'$ end of one nucleotide and another fluorophore linked to the $5'$ end of the second oligonucleotide. In the unhybridized state the donor–acceptor pair also gives low fluorescence background. When there are sufficient amplified templates present, the two oligonucleotide probes are hybridized to the template adjacently to each other (head-to-tail), which brings the donor and acceptor into close proximity to enhance FRET efficiency. The donor fluorophore is excited and the fluorescence signal from the acceptor fluorophore is detected.

4.4
Scorpion Primers and Shared Stem Molecular Beacons

More recently, a variety of new probe designs have been explored for further improvement of the sequence-specific probes described above on the detection sensitivity of quantitative real-time PCR. Scorpion probes are self-probing combinations of primer and probe [28]. The probe and primer are separated by a PCR blocker to prevent construction of a double strand in the probe region. The primer segment binds in the first annealing phase followed by extension. During a second denaturing and annealing the probe portion can then bind to the newly synthesized target on the same strand. Detection of a target sequence is converted into an intramolecular event with improved kinetics and thermodynamics. The original variation featured a stem–loop type of probe like a molecular beacon with the donor fluorophore and acceptor in close proximity. When the probe is bound to the target the acceptor is somewhat removed from the fluorophore, but still in the vicinity. So a more sensitive variation was developed wherein the acceptor was on a second oligonucleotide complementary to the probe sequence [38]. This is known as a duplex scorpion and upon denaturation the acceptor is released. The link between the primer and probe automatically brings the probe into the proximity of the target and is always available for binding. This links amplification with detection in a 1:1 fashion which is not guaranteed with other probe systems, especially with hybridization FRET probes that require two separate bindings to adjacent segments of the same target. The proximity of target to probe was believed to play a role in the performance of a Scorpion probe as compared to TaqMan or beacon probes when running very fast cycling

times [39]. Scorpions have shown utility for the detection of splice variants and mutation detection [39, 40].

Additionally, Kong and coworkers reported shared-stem molecular beacon probes that combined properties of a TaqMan probe (cleavage) and a conventional molecular beacon (stem) [41]. The authors have shown that the signal-to-background ratios are superior to that of conventional molecular beacons using this probe design strategy. Understandably, fluorescence from a fluorophore cleaved from a nucleotide probe ought to be greater than a fluorophore separated from an acceptor by ∼20 nucleic bases like in the case of a conventional molecular beacon.

4.5
Nucleotide-Based Quenching

It is well known that guanosine and guanine cause fluorescence quenching of many commonly used fluorescent dyes, such as fluorescein, coumarin, BODIPY FL, TAMRA, JOE, HEX, TET, ROX, and some of the Alexa dyes [42, 43]. The quenching mechanisms were suggested to be due to photoinduced electron transfer from guanine to the singlet excited state of dye molecules [42, 44]. The degree of quenching depended on various factors, including guanine position relative to the fluorophore attachment site, number of guanines, and the attachment site of the fluorophore in the oligonucleotide (including attachment chemistry). The change in fluorescence intensity attributed to guanine quenching has been exploited to develop novel detection assays for DNA and RNA molecules [18, 29, 45, 46]. One tactic executed by LUX™ fluorogenic primer technology from Invitrogen is to design a molecular beacon primer with the labeling site of a fluorophore in the hairpin region and opposite to several guanosine residues [18]. This design results in highly quenched fluorescence prior to PCR. When the molecular beacon primer is open for the extension during PCR, the fluorescence from the fluorophore is restored.

4.6
Probe Design Issues and Validation

Commonly used, sequence-specific oligonucleotide probes are described above for quantitative real-time PCR. These oligonucleotide probes are generally required for multiplex real-time PCR applications. In order to achieve optimal detection sensitivity, knowledge of the advantages and limitations of each probe design is also required. Below we will use our experimental results to show likely problems associated with some probe design strategies.

In the following study, we investigated three probe design strategies commonly used in quantitative PCR for sensitivity in detection of the PCR amplicon [47]. A plasmid with a 120 base pair insert served as the DNA template. The probes included TaqMan, conventional molecular beacon (MB),

Table 1 Oligonucleotide sequences

Name	Fluorophore	Sequence
Amplicon	None	5′ AGGACGTGGACCAGAGATCGAATGACCATCGTG TGCTGACTCCAGAGGTTGCAGTCAGCGAGTGCA TCAGGTGTTGTAGCCTGATCCCTGTTCCGAAGT ACCTATCGTCGAGCGGTCTGT 3′
Forward primer	None	5′ ACAGACCGCTCGACGATAGG 3′
Reverse primer	None	5′ AGGACGTGGACCAGAGATCG 3′
TaqMan	5′-Fluorescein 3′-Rhodamine	5′ ACTTCGGAACAGGGATCAGGCTACA 3′
ATssMB	5′-Fluorescein 3′-Dabsyl	5′ ACTTCGGAACAGGGATCAGGCTACAccgaagt 3′
GCssMB	5′-Fluorescein 3′-Dabsyl	5′ CGGAACAGGGATCAGGCTACAACAgttccg 3′
MB	5′-Fluorescein 3′-Dabsyl	5′ ccgccCTCTGGAGTCAGCACACGATGGTCAggcgg 3′
GC-TaqMan	5′-Fluorescein 3′-Rhodamine	5′ CGGAACAGGGATCAGGCTACAACAC 3′
TaqssMB	None	5′ AGGTGTTGTAGCCTGATCCCTGTTCCGAAGTACC TAT 3′
CompMB	None	5′ ATCGAATGACCATCGTGTGCTGACTCCAGAGGT TGCAGTCAGCGAGTGCATCAGGTGTTGTAG 3′

and shared-stem molecular beacon (ATssMB and GCssMB). The shared-stem beacon probe briefly described above [41] combines the properties of a Taq-Man probe and a conventional molecular beacon. The sequences of the primers, the real-time PCR amplicon, and various PCR probes are given in Table 1 together with two control oligonucleotides, TaqssMB and CompMB. The lengths and locations of the primers and probes with respect to the amplicon are shown in Fig. 3. With the use of both TaqMan and shared-stem molecular beacon probes, signal amplification relies on hybridization with the amplicon and hydrolysis of the probe by the 5′-exonuclease activity of
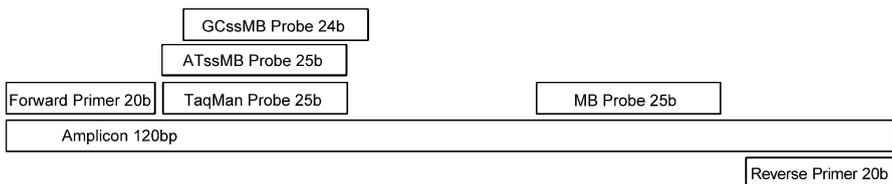
Fig. 3 The positions and lengths of various real-time PCR probes and forward and reverse primers with respect to the amplified region of the model DNA plasmid. The length includes only the regions involved in hybridization

Taq DNA polymerase (55 °C); therefore, these probes were placed close to the forward primer to enhance hydrolysis efficiency. For the molecular beacon probe, the final signal depends on the amplicon concentration and hybridization efficiency with the amplicon. In this case the molecular beacon probe is displaced from the target by Taq DNA polymerase (72 °C). The location of the probe on the target was therefore positioned some distance from the primer. The thermal cycling profiles using these probes were different to reflect the differences in the nature of the probes [47].

Figure 4A shows fluorescence intensities after completion of PCR (gray columns) for the four PCR probes. The black columns in the same figure show the initial fluorescence background averaged over the first five PCR cycles. To account for possible (1) unequal concentrations of probes and/or (2) differences in fluorescence quantum yields of fluorescein in each case due to the microenvironment induced by the nearby nucleotide sequence, the signal-to-background ratio (S/N) was calculated and is displayed in Fig. 4B for comparison of the four probes. The ratio trails in the following order: MB > GCssMB > ATssMB > TaqMan. The conventional molecular beacon probe, MB, gives a low fluorescence background when compared to a TaqMan probe in that fluorescence from the fluorophore is highly quenched by the adjacent quencher as seen in Fig. 4A (black column). Additionally, the guanine bases in the stem portion of the beacon quench the fluorescence of fluorescein. The amount of fluorescence quenching is, in general, proportional to the number of nearby guanine bases (in the region of five to six bases) [43, 46, 48]. Based on these principles, we expected the fluorescence background of the three molecular beacon probes to be in the order of MB < GCssMB < ATssMB. The fluorescence background from GCssMB (Fig. 4A) is surprisingly the lowest among the three beacon probes used in the study. On the other hand, with the use of TaqMan, ATssMB, and GCssMB probes the signal enhancement is critically dependent on the hydrolysis activity of the polymerase during PCR. The final signals after PCR should be comparable for the three probes assuming 100% cleavage efficiency (a single nucleic base conjugated with a fluorescein). Yet, they are very different (Fig. 4A). The signal from ATssMB is the highest and that from GCssMB is the lowest. The fluorescence signals of the post-PCR filtrates obtained by using Microcon YM-3 centrifugal filter devices (molecular weight cutoff of 3000 Da, ten single-stranded nucleotides) are very close to those after PCR, inferring that the three probes are lysed during PCR to be equal to or smaller than ten single-stranded nucleotides in size.

By design, the GCssMB probe should give a better signal-to-background ratio than the ATssMB probe if it is hydrolyzed completely during the PCR and obeys the quenching rule by the number of guanine bases in the stem portion. We measured fluorescence quantum yields of the post-PCR filtrates which are given in Table 2 for TaqMan, ATssMB, and GCssMB probes. The yields for TaqMan and ATssMB probes are relatively close. Although lower
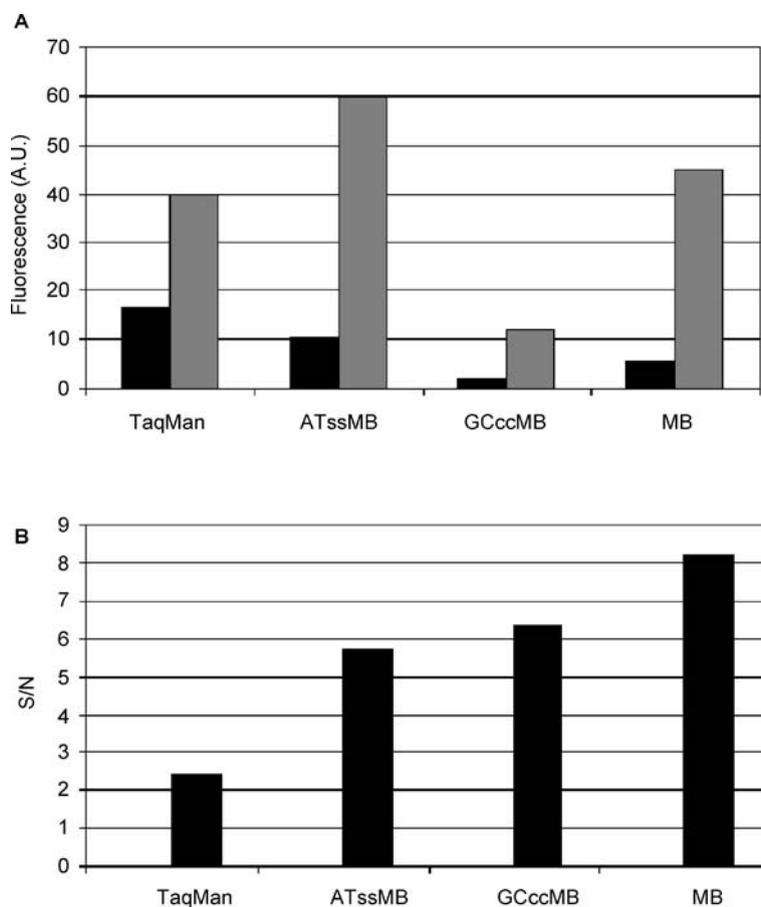
Fig. 4 A Fluorescence signals after completion of PCR (*gray columns*) for various real-time PCR probes. The black columns show the initial fluorescence background averaged over the first five PCR cycles. AU, arbitrary units. **B** Signal-to-background ratios (S/N) obtained using the data given in **A** for the four real-time PCR probes

than expected, it is evident that hydrolysis cleavage takes place during PCR. The yield for GCssMB is, nonetheless, much lower than for the other two. When a GCssMB probe is hybridized to the amplicon, its location is shifted from the primer by four nucleic acid bases more than ATssMB and TaqMan probes. We synthesized a control probe, GC-TaqMan (see Table 1), which has the identical sequence at the 5′ end as the GCssMB probe and no 3′ end stem sequence, to verify if the hydrolysis reaction does indeed take place during real-time PCR. The quantum yield determined for the post-PCR filtrate is 0.59 using GC-TaqMan as the probe. This suggests that the polymerase can effectively cleave the probe and result in an increase of the fluorescence signal because of physical separation of the fluorophore from the quencher.

Table 2 Relative fluorescence quantum yields determined for control samples and filtrates after PCR

	Sample	Quantum yield[b]
Control	dC-fluorescein	0.81
	dA-fluorescein	0.81
	dCG-fluorescein	0.20
	dCGG-fluorescein	0.23
	dCGGA-fluorescein	0.42
	TaqMan	0.19
	TaqMan/TaqssMB	0.65
Probe and duplex with complementary strand[a]	ATssMB	0.081
	ATssMB/TaqssMB	0.78
	GCssMB	0.028
	GCssMB/TaqssMB	0.43
	MB	0.050
	MB/CompMB	0.64
	GC-TaqMan	0.11
	GC-TaqMan/TaqssMB	0.49
Samples after enzymatic digestion	GCssMB + SVP	0.75
	GCssMB + BSPD	0.77
	GCssMB + SVP + BSPD	0.71
Post-PCR filtrate	TaqMan	0.38
	ATssMB	0.47
	GCssMB	0.12
	GC-TaqMan	0.59

[a] The samples in 20 mM Tris-HCl, pH 8.4, 50 mM KCl, 2 mM $MgCl_2$ went through the following protocol: 25 °C for 30 s, 95 °C for 2 min, then decreasing the temperature to 25 °C at the rate of 0.2 °C/s, incubation for 8 min at 25 °C
[b] The quantum yields were averaged over several experimental repeats with a standard deviation of less than 5% for the control, probe alone, and duplexes with the complementary strand and samples after enzymatic digestion, and with standard deviations of $\leq 20\%$ for post-PCR filtrates

Melting curve measurements were then performed to ascertain that GC-ssMB behaved similarly to ATssMB and was able to hybridize to its template. The obtained T_m values for both GCssMB (60.5 °C) and ATssMB (58.8 °C) are similar and 8–10 °C lower than those of their duplexes with the complementary target (TaqssMB): 68.4 °C and 69.0 °C for GCssMB duplex and ATssMB duplex, respectively. These temperatures are generally consistent with the probe design strategies. The results imply that GCssMB and ATssMB should behave similarly in real-time PCR and be able to hybridize to the complementary strand.

We further asked the question whether C-linked fluorescein resulting from the complete hydrolysis of the GCssMB probe would be quenched. Both dC-fluorescein and dA-fluorescein were synthesized to serve as controls. Their

fluorescence quantum yields measured against the reference standard are the same (0.81) and given in Table 2. We measured the quantum yields of GCssMB alone in Tris buffer, pH 8.4, and GCssMB probe digested by two different enzymes either separately or jointly (Table 2). Enzymatic digestion by snake venom phosphodiesterase (SVP) starts from the $5'$ end of the nucleotides and digestion catalyzed by bovine spleen phosphodiesterase (BSPD) originates from the $3'$ end of the nucleotides. The yields for digested GCssMB are close to each other and above 0.70, inferring that fully cleaved GCssMB should fluoresce strongly. Three additional control samples, dCG-fluorescein, dCGG-fluorescein, and dCGGA-fluorescein, were made to show the likely outcomes of partial hydrolyses of GCssMB serving as the probe in PCR. The fluorescence quantum yields of these controls are given in Table 2. The yields for dCG-fluorescein (0.20) and dCGG-fluorescein (0.23) are about four times lower than for dC-fluorescein (0.81), and the yield of dCGGA-fluorescein (0.42) is about half of that of dC-fluorescein. These results point out that a low fluorescence signal after PCR using GCssMB as the probe is most likely due to partial hydrolysis of the probe. Although the quantum yield determined for GCssMB after PCR (0.12) is much lower than anticipated, it is more than four times higher than that of GCssMB in the stem–loop state (0.028). When a GCssMB probe was hybridized to its complementary oligonucleotide, TaqssMB, the quantum yield of the formed duplex (GCssMB/TaqssMB) was measured to be 0.43. This yield is much higher than that after PCR (0.12). The measured yield (0.43) in the duplex form is comparable to that of the duplex GC-TaqMan/TaqssMB (0.49) (Table 2) due to the same microenvironment fluorophores experienced in both cases. Interestingly, the quantum yield of the four PCR probes increases in the order of GCssMB < MB < ATssMB < TaqMan. The trend is the same as that shown in Fig. 4A (black columns).

It is worth noting that the control probe (GC-TaqMan) would be a better probe than TaqMan when comparing the quantum yields of probes alone and post-PCR filtrates (Table 2). The fluorescence signal increases fivefold after PCR for GC-TaqMan and about twofold for TaqMan. The results strongly suggest that one could utilize surrounding nucleotide sequences to improve assay sensitivities when designing PCR probes.

We also prepared a tenfold dilution series of the preamplified DNA construct (1×10^{13}/μL) to compare the sensitivity of various PCR probes. With the same amount of starting material, the signal difference between the second and the first PCR amplification cycles is likely to show the sensitivity of the probe in cases where there is an observable signal difference between one PCR cycle and the next cycle. Figure 5 displays differences in measured fluorescence signals as a function of the concentration (logarithmic copy numbers) of the starting construct for TaqMan (a), ATssMB (b), GCssMB (c), and MB (d). With a starting copy number of 1×10^{12}/μL, the signal difference between the second and first amplification cycles is distinguishable from that of less starting material, for instance, 1×10^{11}/μL using MB, ATssMB, and
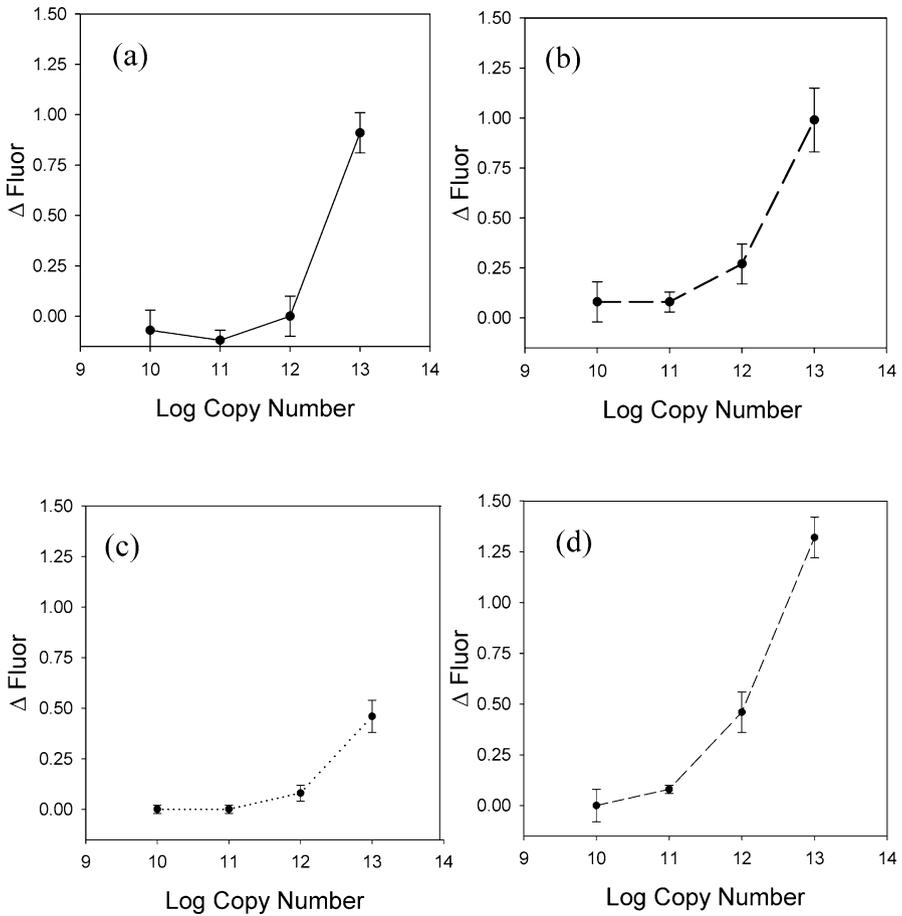
Fig. 5 Differences in fluorescence signals between the second and the first PCR amplification cycles as a function of the concentration (copy number) of the starting amplicons for TaqMan (**a**), ATssMB (**b**), GCssMB (**c**), and MB (**d**). The plots include the standard deviations from nine replicates for each concentration

GCssMB probes. Due to an intrinsic high fluorescence background associated with the TaqMan probe, the signal difference was not significant enough to differentiate the starting material from 1×10^{12} to 1×10^{11} copy/μL. The overall sensitivities for the four probe types are in the order of MB > ATssMB > GCssMB > TaqMan. The sensitivity result is, in general, consistent with that of the signal-to-background ratio shown in Fig. 4B.

Two key points can be learned from this study. One is that the complete hydrolysis generally assumed for the TaqMan probe strategy is not likely to be true. Second, in order to increase the detection sensitivity and signal-to-background ratio of real-time PCR, it is critical to decrease the fluorescence

background of probes through careful placement of reporting fluorophores in the oligonucleotide microenvironment.

The second example is dedicated to the issue of guanine-induced quenching, which can be especially problematic in detection methods employing FRET as decreases in the donor fluorescence could be due to both resonance energy transfer and quenching by the microenvironment. Since fluorescein (FAM) and Alexa-488 are commonly used donor fluorophores [26, 49], for instance, with the use of LightCycler technology, we investigated the influence of the overhang region of the complementary strand on the resulting fluorescence from a hybridizing probe [48].

A series of target oligonucleotides, each with a unique 3′ overhang (four bases long), were hybridized to either 5′ fluorescein or Alexa-488 labeled probes, and the changes in fluorescence intensity and anisotropy were monitored. The four-base overhang serves as a good model for target molecules analyzed using real-time PCR in that significant quenching was observed in the presence of guanine bases in the overhang region, close to the fluorophore labeling nucleotide [29, 46]. The probe sequence was derived from the genome of the bacterium *Bacillus globigii*, and is detailed in Table 3 to-

Table 3 Nomenclature and base sequences of the oligonucleotides used in this study

Annotation	Sequence
Probes	
Alexa probe	5′-/**Alexa-488**/TGC GCC CAT TTT TCA AGC TGC G-3′
Fl probe	5′-/**Fluorescein**/TGC GCC CAT TTT TCA AGC TGC G-3′
Target [a]	
No overhang	5′ –CGC AGC TTG AAA AAT GGG CGC A-3′
TTGT	5′ –CGC AGC TTG AAA AAT GGG CGC ATG TT-3′
TGTT	5′ –CGC AGC TTG AAA AAT GGG CGC ATT GT-3′
GTTT	5′ –CGC AGC TTG AAA AAT GGG CGC ATT TG-3′
TTTG	5′ –CGC AGC TTG AAA AAT GGG CGC AGT TT-3′
GGTT	5′ –CGC AGC TTG AAA AAT GGG CGC ATT GG-3′
TGTG	5′ –CGC AGC TTG AAA AAT GGG CGC AGT GT-3′
GTGT	5′ –CGC AGC TTG AAA AAT GGG CGC ATG TG-3′
TTGG	5′ –CGC AGC TTG AAA AAT GGG CGC AGG TT-3′
GGGT	5′ –CGC AGC TTG AAA AAT GGG CGC ATG GG-3′
TGGG	5′ –CGC AGC TTG AAA AAT GGG CGC AGG GT-3′
AAAA	5′ –CGC AGC TTG AAA AAT GGG CGC AAA AA-3′
CCCC	5′ –CGC AGC TTG AAA AAT GGG CGC ACC CC-3′
TTTT	5′ –CGC AGC TTG AAA AAT GGG CGC ATT TT-3′
GGGG	5′ –CGC AGC TTG AAA AAT GGG CGC AGG GG-3′

[a] The "target" annotation is given as the sequence of the 3′ overhang region (four bases) read from the 3′ to 5′ end. Bold font in the sequences designates a 5′ covalently bound fluorophore attached through an aminohexylphosphate linker
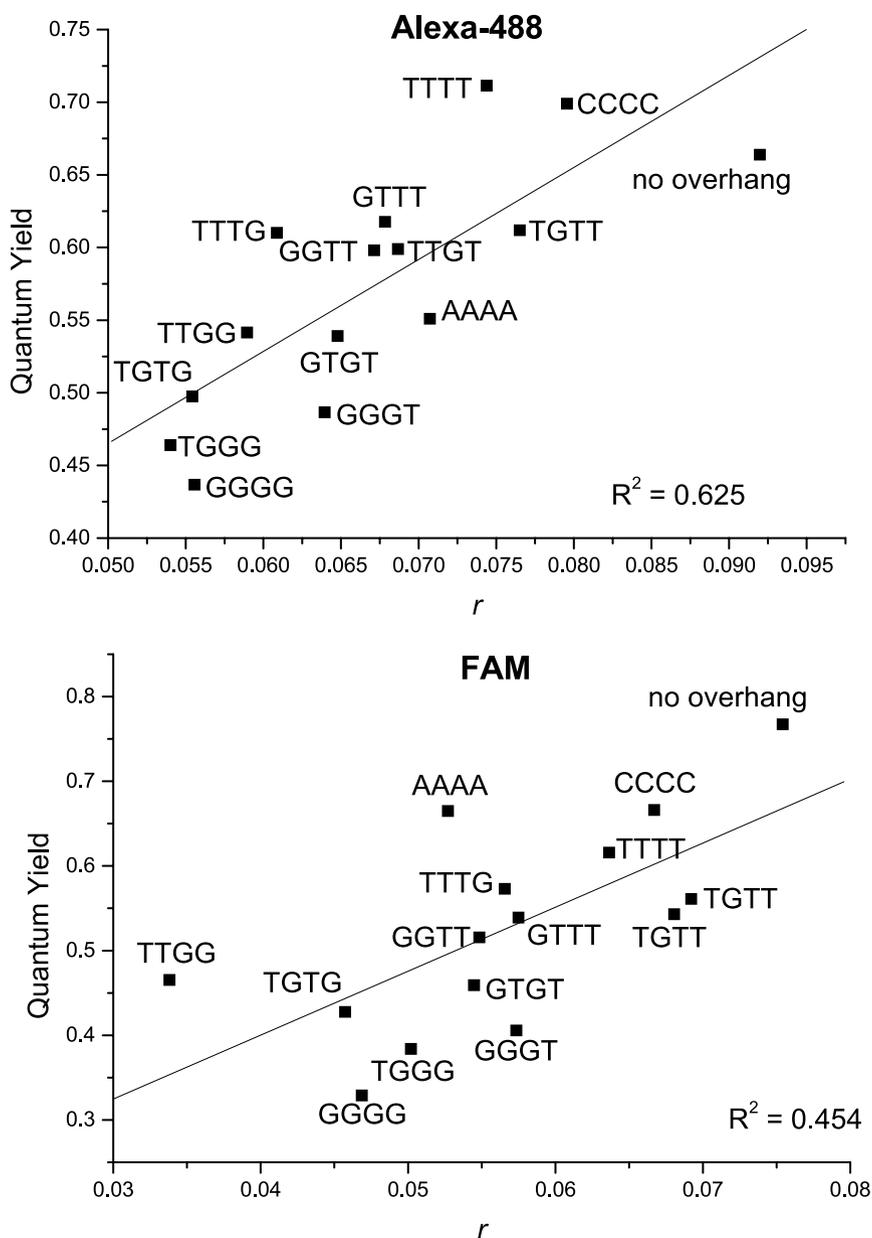
Fig. 6 The relationship between fluorescence quantum yield and anisotropy for the hybridization reactions employing Alexa-488- and FAM-labeled probes. The anisotropy data for each hybridized oligonucleotide shown is mostly the average from two independent reactions (four repeats for the TTTT, TTTG, and GGGG incorporated duplexes), where each spectrum was recorded in duplicate, generating S.E.M. values typically <10% of the total r value

gether with the target sequences. All sequences were analyzed using MFOLD Web Server (Version 3.1) [50] to ensure that potential secondary structures did not complicate the results. We found that the number of guanine bases in the overhang region of the target oligonucleotides is proportional to the amount of fluorescence quenching observed for both the FAM and Alexa-488 dyes (Fig. 6). FAM appeared to be more sensitive to guanine-induced quenching with three and four guanine bases resulting in a greater than twofold decrease in the quantum yield of the fluorophore compared to the no-overhang target. In addition, we found that adenine bases caused fluorescence quenching of the Alexa-488-labeled probe, whereas the FAM-labeled probe appeared insensitive. The quenching data, generated with the steady-state fluorescence measurements, also displayed a linear correlation with those obtained using a fluorescent thermal cycler, suggesting the applicability to real-time PCR measurements (data not shown). Anisotropy data from the series of duplexes correlated with the fluorescence quantum yield (Fig. 6), suggesting that quenching was accompanied by increased dye mobility.

Nazarenko and colleagues [43] found that fluorescence quenching of fluorescein that was attached next to the 3′ end of the probe oligonucleotide by a 5′ one to two guanine base overhang on the complementary target strand was less than that by a terminal G-C pair, though the magnitude of quenching was still significant. Comparison with most reported data is problematic due to the differences in oligonucleotide sequence and furthermore because the data are often not quantitative, i.e., are expressed relative to the single-stranded probe. Our study and other reported work point out that, while designing nucleotide probes for real-time PCR, one needs to pay special attention to about four to five nucleotide bases near the fluorophore labeling nucleotide either at the 3′ end or 5′ end of an oligonucleotide. Even in the case of designing hybridization probes, where a one to five base separation between donor and acceptor is recommended by the manufacturer with the use of LightCycler technology, one should still be able to move donor and acceptor nucleotides around to avoid the quenching effect and enhance energy transfer efficiency. A larger separation distance between the donor–acceptor pair may still allow for adequate transfer efficiency [49] in quantitative real-time PCR.

5
Conclusions

There is a variety of real-time quantitative PCR equipment platforms and amplification fluorescence detection strategies combined with a basic amplification protocol. The diversity of fluorescent tools that are available offers options for many different types of detections. Validation of the fluorescent probe for a specific detection is an important part of the validation of a PCR protocol.

For trace detections the sensitivity of the detection is critical. An example is the quantification of the adventitious presence of genetically modified organisms (GMOs) in grain or food products. Validation of a PCR method also involves the determination of the limit of detection (LOD) and the limit of quantification (LOQ). The sensitivity of the fluorescent probe contributes to the LOD and LOQ. How specific probe types work is fairly straightforward, but as we have tried to convey in this chapter, the performance of a specific probe in the detection of an amplicon should not be assumed. Is there sufficient hydrolysis of a TaqMan-style probe using the 5'-nuclease assay? Is the background fluorescence of a probe significantly lowering the signal-to-noise ratio? Will the probe–quencher combination of a molecular beacon significantly affect the T_m of the probe? Is the design of the assay sufficiently robust to perform if there are slight variations in the performance of the thermocycler platform or variations in the reagent mix? Does the melting curve analysis with SYBR Green detection show all the products? Analysis of the performance of the fluorescent probe as part of the validation process in method development will pay dividends in accuracy and precision of the quantitative PCR assay.

References

1. Saiki RK, Scharf S, Faloona FA, Mullis KB (1985) Science 230:1350
2. Saiki RF, Gelfand DH, Stoffel S, Scharf S, Higuchi R, Horn GT, Mullis KB, Erlich HA (1988) Science 239:487
3. Bustin SA (ed) (2004) A–Z of quantitative PCR. International University Line, La Jolla
4. Edwards K, Logan J, Saunders N (eds) (2004) Real-time PCR: an essential guide. Horizon Bioscience, Norfolk
5. Meuer S, Wittwer CT, Nakagawara K-I (eds) (1999) Rapid cycle real-time PCR: methods and applications. Springer, Heidelberg
6. Wittwer CT, Herrmann MG, Moss AA, Rasmussen RP (1997) Biotechniques 22:130
7. Higuchi R, Dollinger G, Walsh PS, Griffith R (1992) Biotechnology 10:413
8. Higuchi R, Fockler C, Dollinger G, Watson R (1993) Biotechnology (NY) 11:1026
9. Nakao M, Janssen JWG, Flohr T, Bartram CR (2000) Cancer Res 60:328
10. Dhar AK, Roux MM, Klimpel KR (2001) J Clin Microbiol 39:2835
11. Vandesompele J, De Paepe A, Speleman F (2002) Anal Biochem 303:95–98
12. Mouillesseaux KP, Klimpel KR, Dhar AK (2003) J Virol Methods 111:121
13. Karsai A, Muller S, Platz S, Hauser M-T (2002) Biotechniques 32:790
14. Monis PT, Giglio S, Saint CP (2005) Anal Biochem 340:24
15. Giglio S, Monis PT, Saint CP (2003) Nucleic Acids Res 31:e136
16. Tyagi S, Kramer FR (1996) Nat Biotechnol 14:303
17. Szuhai K, Sandhaus E, Kolkman-Uljee SM, Lemaitre M, Truffert JC, Dirks RW, Tanke HJ, Fleuren GJ, Schuuring E, Raap AK (2001) Am J Pathol 159:16
18. Nazarenko I, Lowe B, Darfler M, Ikonomi P, Schuster D, Rashtchian A (2002) Nucleic Acids Res 30:e37
19. Lie YS, Petropoulos CJ (1998) Curr Opin Biotechnol 9:43
20. Barragan E, Bolufer P, Moreno I, Martin G, Nomdedeu J, Brunet S, Fernandez P, Rivas C, Sanz MA (2001) Leuk Lymphoma 42:747

21. Marras SAE, Kramer FR, Tyagi S (1999) Genet Anal Biomol E 14:151
22. Breen G, Harold D, Ralston S, Shaw D, St Clair D (2000) Biotechniques 28:464
23. Heid CA, Stevens J, Livak KJ, Williams PM (1996) Genome Res 6:986
24. Lewin SR, Vesanen M, Kostrikis L, Hurley A, Duran M, Zhang L, Ho DD, Markowitz M (1999) J Virol 73:6099
25. Szuhai K, Ouweland J, Dirks R, Lemaitre M, Truffert J, Janssen G, Tanke H, Holme E, Maassen J, Raap A (2001) Nucleic Acids Res 29:e13
26. Eckert C, Landt O, Taube T, Seeger K, Beyermann B, Proba J, Henze G (2000) Leukemia 14:316
27. Cardullo RA, Agrawal S, Flores C, Zamecnik PC, Wolf DE (1988) Proc Nat Acad Sci USA 85:8790
28. Whitcombe D, Theaker J, Guy SP, Brown T, Little S (1999) Nat Biotechnol 17:804
29. Kurata S, Kanagawa T, Yamada K, Torimura M, Yokomaku T, Kamagata Y, Kurane R (2001) Nucleic Acids Res 29:e34
30. Lakowicz JR (1999) Principles of fluorescence spectroscopy. Plenum Press, New York
31. Marras SAE, Kramer FR, Tyagi S (2002) Nucleic Acids Res 30:e122
32. Holland PM, Abramson RD, Watson R, Gelfand DH (1991) Proc Nat Acad Sci USA 88:7276
33. Kutyavin IV, Afonina IA, Mills A, Gorn VV, Lukhtanov EA, Belousov ES, Singer MJ, Walburger DK, Lokhov SG, Gall AA, Dempcy R, Reed MW, Meyer RB, Hedgpeth J (2000) Nucleic Acids Res 28:655
34. Kulesh DA, Baker RO, Loveless BM, Norwood D, Zwiers SH, Mucker E, Hartmann C, Herrera R, Miller D, Christensen D, Wasieloski LP Jr, Huggins J, Jahrling PB (2004) J Clin Microbiol 42:601
35. Luderer R, Verheul A, Kortlandt W (2004) Clin Chem 50:787
36. Whiley DM, Sloots TP (2006) J Clin Virol 35:81
37. Kennedy B, Arar K, Reja V, Henry RJ (2006) Anal Chem 348:294
38. Solinas A, Brown LJ, McKeen C, Mellow JM, Nicol JTG, Thelwell N, Brown T (2001) Nucleic Acids Res 29:e96
39. Thelwell N, Millington S, Solinas A, Booth J, Brown T (2000) Nucleic Acids Res 28:3752
40. Taveau M, Stockholm D, Spencer M, Richard I (2002) Anal Biochem 305:227
41. Kong D-M, Gu L, Shen H-S, Mi H-F (2002) Chem Commun 8:854
42. Torimura M, Kurata S, Yamada K, Yokomaku T, Kamagata Y, Kanagawa T, Kurane R (2001) Anal Sci 17:155
43. Nazarenko I, Pires R, Lowe RB, Obaidy M, Rashtchian A (2002) Nucleic Acids Res 30:2089
44. Seidel CAM, Schulz S, Sauer MHM (1996) J Phys Chem 100:5541
45. Knemeyer JP, Marme N, Sauer M (2000) Anal Chem 72:3717
46. Crockett AO, Wittwer CT (2001) Anal Biochem 290:89
47. Wang L, Blasic JR Jr, Holden MJ, Pires R (2005) Anal Biochem 344:257
48. Noble JE, Wang L, Cole KD, Gaigalas AK (2005) Biophys Chem 113:255
49. Wang L, Gaigalas AK, Blasic JR Jr, Holden MJ, Gallagher DT, Pires R (2003) Biopolym (Biospectrosc) 72:401
50. Zuker M (2003) Nucleic Acids Res 31:3406